

2017

# Advancing Automated Methods for MicroRNA Profiling

Kia N. Zellars

*University of South Carolina*

Follow this and additional works at: <https://scholarcommons.sc.edu/etd>



Part of the [Biomedical Engineering and Bioengineering Commons](#)

---

## Recommended Citation

N. Zellars, K. (2017). *Advancing Automated Methods for MicroRNA Profiling*. (Doctoral dissertation). Retrieved from <https://scholarcommons.sc.edu/etd/4421>

This Open Access Dissertation is brought to you for free and open access by Scholar Commons. It has been accepted for inclusion in Theses and Dissertations by an authorized administrator of Scholar Commons. For more information, please contact [dillarda@mailbox.sc.edu](mailto:dillarda@mailbox.sc.edu).

# ADVANCING AUTOMATED METHODS FOR MICRORNA PROFILING

by

Kia N. Zellars

Bachelor of Science  
University of Georgia, 2010

---

Submitted in Partial Fulfillment of the Requirements

For the Degree of Master of Science in

Biomedical Science

School of Medicine

University of South Carolina

2017

Accepted by:

Francis Spinale, Director of Thesis

Daping Fan, Reader

Michael J. Friez, Reader

Jay D. Potts, Reader

Homayoun Valafar, Reader

Cheryl L. Addy, Vice Provost and Dean of the Graduate School

© Copyright by Kia N. Zellars, 2017  
All Rights Reserved.

## ACKNOWLEDGEMENTS

My sincere acknowledgment and appreciation to my advisor, Dr. Francis Spinale, for his invaluable assistance, guidance, and expertise that has bolstered my scientific knowledge base as well as impacted my individual development as a researcher. I would like to thank my thesis committee members: Dr. Daping Fan, Dr. Michael J. Friez, Dr. Jay Potts, and Dr. Homayoun Valafar for their constructive critiques. I express my sincere appreciation to all my lab-mates and colleagues for their continued encouragement and assistance. Giving utmost thanks to my family and my friends for their unconditional love, understanding, unwavering support, and enthusiastic motivation throughout my life's journey.

## ABSTRACT

The widespread influence of miRNAs in many biological processes and characteristic changes in expression profiles make them potential biomarkers for a range of diseases. With recent discoveries highlighting the enrichment of particular circulating miRNAs in plasma under pathological conditions, there has been a push for technological advances in miRNA profiling studies as a diagnostic tool.

A standardized, automated, high-throughput method for miRNA isolation from human plasma samples was developed in this study. Samples were subject to full miRNome profiling utilizing RT-qPCR. These unique findings demonstrate that developing a distinct miRNA biomarker profile for heart failure patients is feasible and holds potential diagnostic value.

## TABLE OF CONTENTS

ACKNOWLEDGEMENTS .....	iii
ABSTRACT .....	iv
LIST OF TABLES.....	vi
LIST OF FIGURES .....	vii
LIST OF ABBREVIATIONS .....	viii
CHAPTER 1: INTRODUCTION .....	1
1.1 OVERVIEW AND CLINICAL SIGNIFICANCE.....	1
1.2 CURRENT METHODS AND LIMITATIONS.....	3
1.3 PROJECT SCOPE/SPECIFIC AIMS.....	5
CHAPTER 2: ASSESSMENT OF AUTOMATED MIRNA ISOLATION .....	7
2.1 METHODS.....	7
2.2 RESULTS.....	8
CHAPTER 3: ASSESSMENT OF AUTOMATED MIRNA PROFILING .....	12
3.1 METHODS.....	12
3.2 RESULTS.....	12
CHAPTER 4: CONCLUSION .....	23
4.1 THESIS CONCLUSION.....	23
4.2 LIMITATIONS.....	24
4.3 FUTURE WORK.....	25
REFERENCES .....	30

## LIST OF TABLES

Table 3.1 Human Cardiovascular miRNA PCR Array-Fold Change Distribution.	14
Table 3.2 Human mirNome PCR Array-Fold Change Distribution .....	15

## LIST OF FIGURES

Figure 2.1 cDNA Synthesis and PCR Array Setup Workflow .....	9
Figure 2.2 RT-qPCR Workflow.....	10
Figure 2.3 C.Elegans mir-39-3p RT-qPCR Standard Curve .....	11
Figure 3.1 Human Cardiovascular Disease miRNA PCR Array CV Distribution .	19
Figure 3.2 Human Cardiovascular Disease miRNA PCR Array Ct Distribution...	20
Figure 3.3 Human miRNome PCR Array PCR Array Ct Distribution.....	21
Figure 3.4: Functional Grouping of miRNAs with >10-fold change .....	22
Figure 4.1: Manual Vs Automated Protocol: Time Efficiency .....	27
Figure 4.2 RT-qPCR Workflow Challenges.....	28

## LIST OF ABBREVIATIONS

BNP/NT-proBNP .....	Brain Natriuretic Peptide/ N-terminal pro brain natriuretic peptide
cDNA .....	Complementary DNA
Ct .....	Cycle Threshold
CV .....	Coefficient of Variation
ddPCR .....	Droplet Digital Polymerase Chain Reaction
EDTA .....	Ethylenediaminetetraacetic acid
HF .....	Heart Failure
miRNA .....	MicroRNA
miRNome .....	Human miRNA Genome
miRTC.....	MicroRNA Reverse Transcriptase Control
mRNA .....	Messenger RNA
PPC .....	Positive PCR Control
RT-qPCR .....	Quantitative Reverse Transcription Polymerase Chain Reaction
snoRNA/snRNA .....	Small Nucleolar RNAs

# CHAPTER 1

## INTRODUCTION

### 1.1 OVERVIEW AND CLINICAL SIGNIFICANCE

Heart failure (HF) is the leading cause of mortality in industrialized countries [26]. HF is the outcome of various myocardial or vascular diseases that ultimately result in insufficient cardiac output to maintain blood circulation throughout the body [2,26,50]. Various congenital and acquired cardiovascular or metabolic diseases such as coronary artery disease, hypertension, and myocardial infarction can lead to the structural and functional impairment of the heart and development of HF [15,20]. HF cannot be determined with a single test [23,31,44]. HF diagnoses are determined collectively by the detection of several clinical symptoms confirmed by imaging and circulating levels of various neurohormones, which includes the routine assessment of BNP/NT-proBNP plasma levels [31,43,37,49]. While the assessment of BNP/NT-proBNP plasma levels as a biomarker for HF diagnoses has significantly improved HF disease management, several complex factors such as obesity and renal function can affect the accuracy of BNP/NT-proBNP as diagnostic tests [8,13,43,38]. This has fueled interest in other possible HF biomarkers such as miRNAs.

MicroRNAs (miRNA) are small noncoding RNAs, approximately 22 nucleotides long, that post-transcriptionally regulate the expression of various

genes by binding to specific messenger RNA (mRNA) transcripts to signal its degradation or inhibition before translation into a protein [17,35]. One miRNA may regulate 100s-1000s of mRNAs, often in the same biological pathway [27,39]. miRNA may act as either positive or negative regulators in various specific signaling cascades or cell mechanisms [35,32]. So far, over 1000 human miRNA sequences have been listed in miRBase (<http://www.mirbase.org>), the definitive repository of identified miRNA sequences and nomenclature system [16,24,32,35]. miRBase is an essential resource for miRNA profiling to include pre-cursor and mature miRNAs.

The mechanism of producing mature miRNAs has been well characterized and should be considered when studying these sequences [32,35,44,49]. The processing of mature miRNA begins with long primary miRNAs (pri-miRNAs) transcripts, which are generally several thousand nucleotides long. Pri-miRNAs then undergo several cleavage steps within the nucleus by the Drosha complex that result in several pre-miRNA (precursor miRNA). Pre-miRNA sequences are hairpin structures, approximately 70-100 nucleotides long. Pre-miRNA is then exported out of the nucleus by Exportin [22]. In the cytoplasm, pre-miRNAs are further modified/cleaved into several distinct mature miRNA sequences by the Dicer protein and loaded onto the RISC complex where they are bound by Argonaute. The RISC complex targets mRNA transcripts for inhibition within the cell [3,22,28] miRNAs can also be exported outside of the cell during this process; however, the exact mechanisms remain unknown [26,45,47]. Recent studies have highlighted the presence of miRNAs in plasma. While miRNAs can

exist freely in plasma, endogenous plasma miRNAs are normally packaged in lipoproteins, exosomes, or associated with other protein complexes such as Argonaute [4,19,32,45,47].

The widespread influence of miRNAs in many biological processes and characteristic changes in expression profiles make them potential biomarkers for a range of diseases including cancer, cardiovascular diseases, metabolic diseases, autoimmune diseases, and more [29,32,36,40]. Recent studies have highlighted the enrichment of particular circulating miRNAs in plasma under pathological conditions [32]. These recent discoveries in miRNA expression have pushed for technological advances in miRNA profiling studies as a diagnostic tool.

## **1.2 CURRENT METHODS AND LIMITATIONS**

The role of miRNAs in cardiac function in the myocardium has been widely studied and defined in animal models [2,26,44]. For example, muscle specific miR-1, muscle specific miR-133a/b, heart specific miR-208a/b, and heart specific miR-499 contribute to myocardial function and are key regulators of cardiac hypertrophy [2,5,6]. Classes of miRNAs have been profiled in human studies; however, heart tissues and circulating miRNA abundance changes were not acquired simultaneously as this is not clinically feasible [44,49]. Due to several confounding limitations and conflicting reports, these present studies do not yet provide sufficient support for the clinical use of miRNAs or provide a distinct HF miRNA profile [14,44,48,49].

In the aforementioned human studies, various liquid biopsy sample types such as blood, plasma, and serum were used. Additionally, variability resulted from different miRNA isolation methods. Currently miRNA can be isolated from cells, fresh tissues, formalin fixed tissues, plasma, serum, and other body fluids [1]. Several commercial systems are available for manual miRNA isolation based chemical extraction using concentrated chaotropic agents, such as guanidine thiocyanate, along with phenol-chloroform followed by solid-phase extraction on silica columns [36]. With normal high-quality miRNA yield from cells and tissues, circulating miRNA exist in lower concentrations in comparison to normal high-quality miRNA yield from cells and tissues. This presents a challenge for the researcher [28,41]. The previously mentioned methods largely target freely circulating miRNA. However, endogenous plasma miRNAs are normally associated with vesicles, exosomes, and other protein complexes [19,36,44,51].

Current manual exosome isolation methods consist of ultracentrifugation or novel exosome affinity based methods [12]. Bound exosomes can then be lysed and miRNA isolation methods carried out. The high concentration of proteins in plasma and different sample processing conditions could greatly alter miRNA content and profiles during isolation methods [25,36,42,44]. For these reasons, consistently efficient methods for miRNA extraction from a large number of liquid biopsy samples remain deficient. As a result, many reported studies have relatively small patient numbers in various HF groups [2,26,44,49]. Therefore, there is a significant need to optimize and develop more automated, high-throughput methods for miRNA isolation from human liquid biopsies.

Additionally, there are several techniques used to measure miRNAs to include RNA sequencing, microarrays, and RT-qPCR [26,36,44]. RT-qPCR is the most well established procedure. Using these methods, different normalization methods and reference genes are reported [25,34,36.44]. Currently, no standardized normalization method for miRNA profiling in liquid biopsies exist. As emerging technologies have only recently become available, not all studies started with a large miRNA panel screen to identify the most differentially expressed miRNAs [36]. Consequently, there is a significant need to standardize miRNA profiling methods for human liquid biopsies with an unbiased approach.

Finally, liquid biopsies are used in a wide range of clinical tests due to noninvasiveness and easy procurement. However, different pathophysiological states could limit biopsy volume and quality. Therefore, using the smallest volume possible for miRNA profiling from the patient is of great importance.

### **1.3 PROJECT SCOPE/SPECIFIC AIMS**

The overall goal of this study will be to develop for the first time a standardized, automated, high-throughput miRNA isolation method from a limited amount of plasma for the first time. The fundamental hypothesis of this project is that a specific and differential plasma miRNA biomarker profile will be identified in heart failure (HF) patients after successfully extracting miRNA using this platform.

*Specific Aim 1:* Isolate freely circulating miRNA using the fully automated

platform from archived human plasma samples (n=3). miRNA extraction efficiency and reproducibility will be validated.

*Specific Aim 2:* Identify distinct plasma miRNA profiles in a relevant clinical HF study to be utilized as a predictive model for biomarker profiling. Using referent control (non-HF) patient samples(n=3) and HF patient samples(n=3), gene expression analyses will be carried out by subjecting isolated miRNA to real-time qPCR arrays that profile the full known human miRNA genome.

Using precise measurements and a suitable patient sample size, results from this project can be translated into relevant disease diagnostic or prognostic tools that can be utilized in various clinical settings.

## CHAPTER 2

### ASSESSMENT OF AUTOMATED MIRNA ISOLATION

#### 2.1 METHODS

*miRNA isolation.* Patient blood samples (referent control: n=3, heart failure: n=3) were collected in EDTA blood collection tubes. They were immediately centrifuged and plasma was stored at  $-80^{\circ}\text{C}$  in 200  $\mu\text{L}$  aliquots until use.

Total RNA was isolated from 200  $\mu\text{L}$  of plasma. 200  $\mu\text{L}$  plasma samples were pre-treated with a phenol-chloroform phase separation. During the pre-treatment separation, samples were spiked with a known amount of synthetic *C. elegans* miR-39-3p sequence (Cat #219610, Qiagen). The obtained aqueous phases of the lysates were transferred to a 2 ml microcentrifuge tube in preparation for automated miRNA extraction. miRNA from pre-treated samples were further isolated using an automated protocol on the QIAcube workstation (Model #9001292, Qiagen) utilizing the miRNeasy Mini Kit (Cat #217004, Qiagen). Isolated miRNA was eluted in 20  $\mu\text{L}$  elution buffer.

*RT-qPCR.* Isolated miRNA was reverse transcribed into a 20  $\mu\text{L}$  cDNA using miScript II RT kit (Cat#218161, Qiagen) with incubation at  $37^{\circ}\text{C}$  for 60 min and  $95^{\circ}\text{C}$  for 5 min. cDNA synthesis is shown in **Figure 2.1**. cDNA was initially diluted 10-fold. The diluted cDNA was then serially diluted, and each dilution was

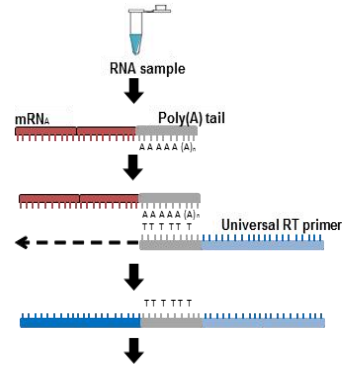
then separately combined with miScript SYBR Green PCR components (Cat#218073, Qiagen) which contains the *C. elegans* mir-39-3p primer for a total of 20  $\mu$ L PCR reaction mix per well. These reaction mixtures were aliquoted in triplicates into predetermined wells of the Rotor-Disc 100. All cDNA synthesis steps and PCR setup were performed by the QIAgility (Model #9001532, Qiagen) using an automated pipetting protocol. Real-time qPCR was performed on the Rotor-Disc 100 by the Rotor-Gene Q real-time PCR cycler (Model #9001570, Qiagen). RT-qPCR workflow is shown in **Figure 2.2**. Rotor-Gene PCR cycling conditions were performed according to manufacturer's suggested protocol and conditions: Activation step-15min @ 95°C; 3-step cycling for 40 total cycles: denaturation- 15s @ 94°C, annealing- 30s @ 55°C, extension 30s @ 70°C; followed by a dissociation (melt) curve analysis. A *Cel*-miR-39 standard curve was generated based on the dilution series. qPCR efficiency was calculated using the formula:  $\text{Efficiency} = 10^{(-1/\text{slope})} - 1$ .

## 2.2 RESULTS

*RT-qPCR*. qPCR analysis showed that *cel*-miR-39-3p exhibited excellent linearity between the target input and measured values in a dynamic range of  $1 \times 10^3$  to  $1 \times 10^6$  copies/ $\mu$ L of input. Furthermore, in this dynamic range, qPCR displayed an estimated 105% PCR efficiency and  $R^2$  values that were close to 1 (0.96–0.99). A representative standard curve is shown in **Figure 2.3**.

Based on *cel*-miR-39-3p Ct values, coefficient of variation(CV) values were determined to be intraplate:  $0.62\% \pm 0.17\%$  and interplate:  $1.95\% \pm 0.43\%$  with a sample miRNA extraction efficiency of  $66.88\% \pm 6.16\%$ .

1. cDNA synthesis by reverse transcription reaction.



2. PCR setup: Combine cDNA, Universal Primer, miScript Primer Assay of interest, and QuantiTect SYBR Green Mastermix. Aliquot mixture across miRNA PCR array.

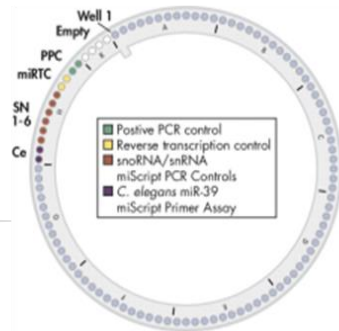
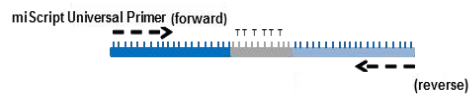
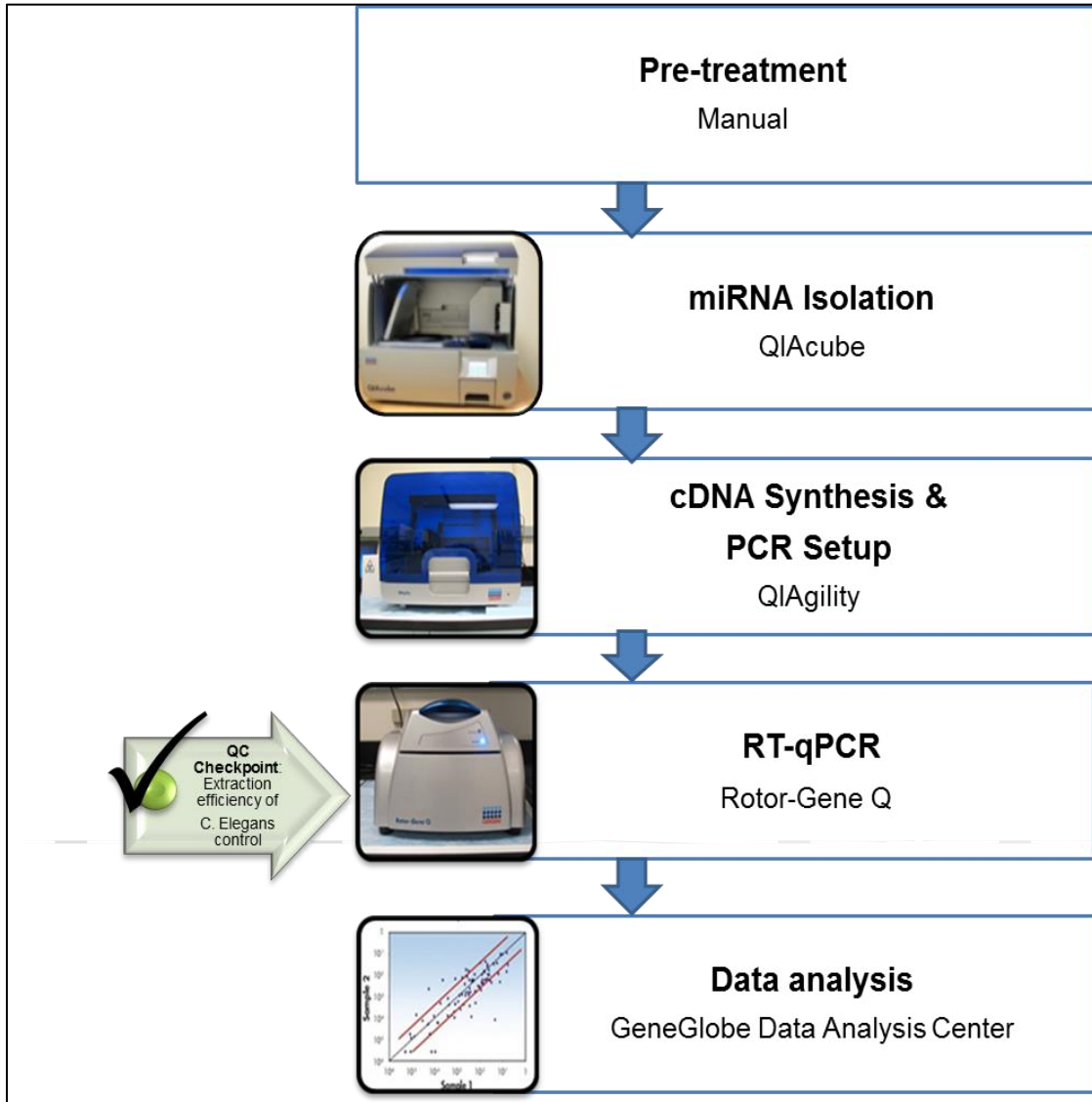
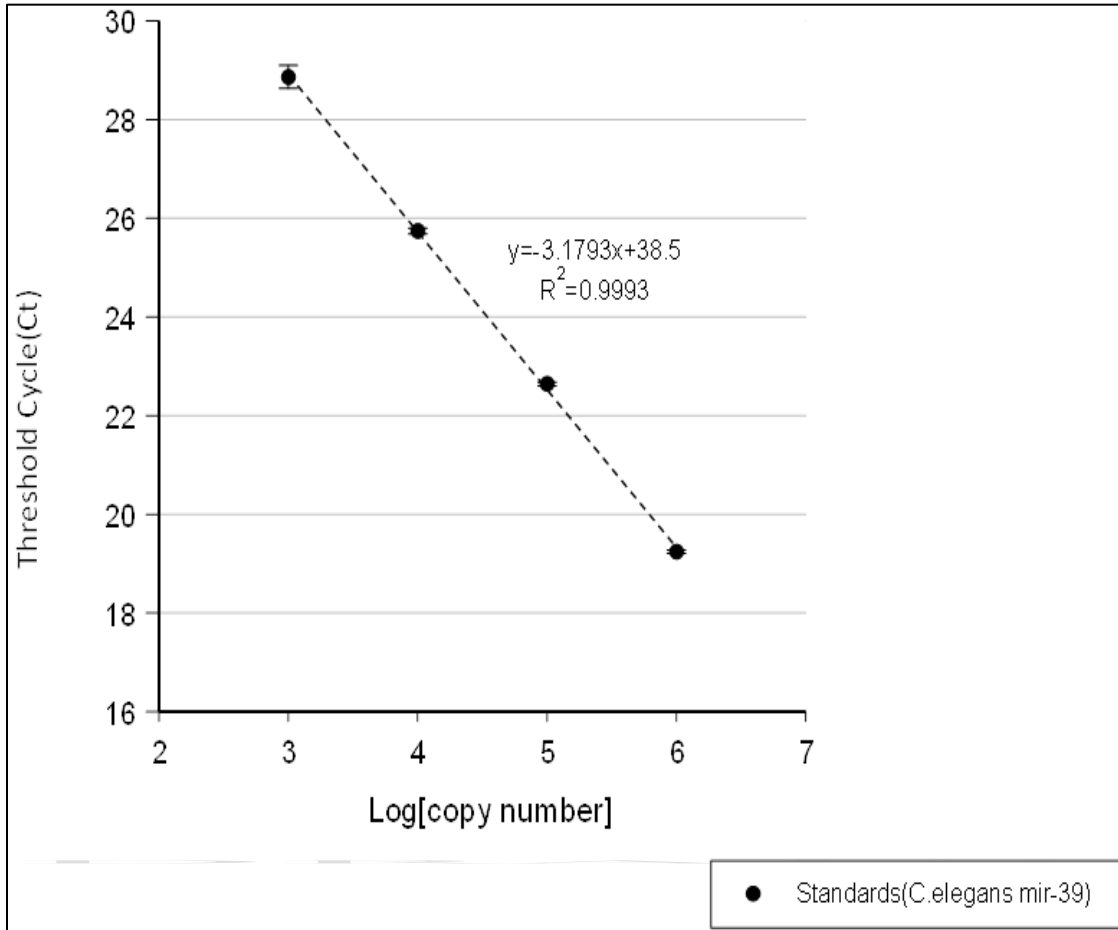


Figure 2.1: cDNA Synthesis and PCR Array Setup Workflow



**Figure 2.2: RT-qPCR Workflow**



**Figure 2.3: C.Elegans mir-39-3p RT-qPCR Standard Curve**

## CHAPTER 3

### ASSESSMENT OF AUTOMATED MIRNA PROFILING

#### 3.1 METHODS

Isolated miRNA was reverse transcribed and RT-qPCR was performed as described previously in section 2.2. Entire human miRNA genome (miRNome) profiling was performed with Human miRNome miScript miRNA PCR Array (Cat#MIHS-113ZR, Qiagen) that analyzes the expression of the 1008 best defined and most abundant miRNAs in the human miRNA. Specific pathway-focused profiling was performed on the Human Cardiovascular Disease miScript miRNA PCR Array (Cat#MIHS-113ZR, Qiagen) that analyzes 84 miRNAs identified as exhibiting altered expression during cardiovascular disease and development. Cel-miR-39-3p was used to normalize miRNAs levels using the  $2^{-\Delta\Delta Ct}$  method. Data analysis was performed in the GeneGlobe Data Analysis Center PCR software (Qiagen).

#### 3.2 RESULTS

There was detectable expression for approximately 88.89% of the 84 miRNAs included in the Human Cardiovascular Disease miScript miRNA PCR Array. Approximately 80% of miRNA sequences on this panel had a CV of <5% as shown in **Figure 3.1**. The distribution of threshold cycling (Ct) values is shown in **Figure 3.2**. Distribution of fold change values are represented in **Table 3.1**.

There was detectable expression for approximately 32.23% of the 1008 miRNAs included in the miRNome miScript miRNA PCR Array. The distribution of threshold cycling (Ct) values is shown in **Figure 3.3**. Distribution of fold change values are represented in **Table 3.2**.

All PCR array PPC values were in range and indicate high quality RNA samples. Furthermore, miRTC values were within range and indicate no inhibition of the reverse-transcription reactions.

**Figure 3.4** shows an emerging distinct miRNA profile of samples tested in this study. Specified functional groups are described by the Cardiovascular Disease miRNA PCR Array which delineates distinct patterns of miRNA expression that correlate with specific cardiovascular disorders. These described patterns are based on studies involving a broad set of cardiovascular disease model systems, clinical tissue samples, and cell lines

**Table 3.1: Human Cardiovascular miRNA PCR Array - Fold Change Distribution**

<b>Fold Change</b>		
<b>2-4(n=5)</b>	<b>4-10 (n=33)</b>	<b>&gt;10 (n=26)</b>
hsa-miR-143-3p	hsa-miR-93-5p	hsa-miR-221-3p
hsa-miR-16-5p	hsa-miR-29b-3p	hsa-miR-210-3p
hsa-miR-22-3p	hsa-miR-486-5p	hsa-miR-30d-5p
hsa-miR-206	hsa-miR-25-3p	hsa-miR-23a-3p
hsa-miR-451a	hsa-miR-145-5p	hsa-miR-183-5p
	hsa-miR-17-5p	hsa-miR-125a-5p
	hsa-miR-27a-3p	hsa-let-7a-5p
	hsa-miR-30e-5p	hsa-miR-26b-5p
	hsa-miR-223-3p	hsa-miR-15b-5p
	hsa-miR-342-3p	hsa-miR-126-3p
	hsa-miR-100-5p	hsa-miR-222-3p
	hsa-miR-208a-3p	hsa-miR-224-5p
	hsa-miR-31-5p	hsa-miR-146a-5p
	hsa-miR-328-3p	hsa-miR-21-5p
	hsa-miR-378a-3p	hsa-let-7e-5p
	hsa-miR-494-3p	hsa-miR-103a-3p
	hsa-miR-92a-3p	hsa-miR-98-5p
	hsa-miR-27b-3p	hsa-miR-181b-5p
	hsa-miR-150-5p	hsa-miR-23b-3p
	hsa-miR-199a-5p	hsa-miR-26a-5p
	hsa-miR-7-5p	hsa-let-7d-5p
	hsa-miR-142-3p	hsa-miR-30c-5p
	hsa-miR-24-3p	hsa-miR-181a-5p
	hsa-miR-130a-3p	hsa-miR-107
	hsa-miR-1-3p	hsa-miR-182-5p
	hsa-miR-423-3p	hsa-let-7f-5p
	hsa-let-7c-5p	
	hsa-miR-18b-5p	
	hsa-let-7b-5p	
	hsa-miR-155-5p	
	hsa-miR-320a	
	hsa-miR-30a-5p	
	hsa-miR-185-5p	

**Table 3.2: Human miRNome PCR Array - Fold Change Distribution**

<b>Fold Change</b>			
<b>0.5(n=4)</b>	<b>2-4(n=111)</b>	<b>4-10 (n=88)</b>	<b>&gt;10 (n=53)</b>
hsa-miR-193a-5p	hsa-miR-125b-5p	hsa-let-7a-3p	hsa-miR-181a-5p
hsa-miR-581	hsa-miR-374b-3p	hsa-miR-1-3p	hsa-miR-181c-5p
hsa-miR-608	hsa-miR-532-5p	hsa-miR-628-3p	hsa-miR-423-5p
hsa-miR-365b-3p	hsa-miR-1255b-5p	hsa-miR-27b-5p	hsa-miR-24-3p
	hsa-miR-3664-5p	hsa-miR-25-3p	hsa-miR-26b-5p
	hsa-miR-4296	hsa-miR-421	hsa-miR-17-5p
	hsa-miR-18a-3p	hsa-miR-342-5p	hsa-miR-181b-5p
	hsa-miR-548t-3p	hsa-miR-628-5p	hsa-miR-224-5p
	hsa-miR-545-5p	hsa-miR-877-3p	hsa-miR-1260a
	hsa-miR-3135a	hsa-let-7c-5p	hsa-miR-425-3p
	hsa-miR-505-5p	hsa-miR-221-5p	hsa-miR-374a-5p
	hsa-miR-551b-3p	hsa-miR-486-5p	hsa-miR-200c-3p
	hsa-miR-548i	hsa-miR-502-3p	hsa-miR-21-5p
	hsa-miR-200b-5p	hsa-miR-877-5p	hsa-miR-107
	hsa-miR-1908-5p	hsa-miR-4286	hsa-miR-222-3p
	hsa-miR-432-5p	hsa-miR-30b-3p	hsa-miR-30e-3p
	hsa-miR-3655	hsa-miR-16-2-3p	hsa-let-7d-3p
	hsa-miR-3157-5p	hsa-miR-4309	hsa-miR-340-3p
	hsa-miR-941	hsa-miR-7-5p	hsa-miR-18a-5p
	hsa-miR-449c-5p	hsa-miR-223-5p	hsa-miR-23a-3p
	hsa-miR-29a-5p	hsa-miR-409-3p	hsa-miR-126-5p
	hsa-miR-29b-2-5p	hsa-miR-1260b	hsa-miR-23b-3p
	hsa-miR-29b-1-5p	hsa-miR-195-5p	hsa-miR-1307-3p
	hsa-miR-148a-3p	hsa-miR-27a-3p	hsa-miR-146b-5p
	hsa-let-7g-3p	hsa-miR-150-5p	hsa-miR-342-3p
	hsa-miR-676-5p	hsa-miR-130b-3p	hsa-miR-339-5p
	hsa-miR-210-3p	hsa-miR-19b-3p	hsa-miR-15b-5p
	hsa-miR-539-5p	hsa-miR-451a	hsa-miR-221-3p
	hsa-miR-1471	hsa-miR-320b	hsa-miR-126-3p
	hsa-miR-187-5p	hsa-miR-2110	hsa-let-7g-5p
	hsa-miR-409-5p	hsa-miR-15b-3p	hsa-miR-146a-5p
	hsa-miR-345-5p	hsa-miR-495-3p	hsa-miR-130a-3p
	hsa-miR-17-3p	hsa-let-7f-5p	hsa-let-7d-5p
	hsa-miR-1909-5p	hsa-miR-22-5p	hsa-miR-103a-3p
	hsa-miR-491-3p	hsa-miR-29a-3p	hsa-miR-652-3p

<b>Fold Change</b>			
<b>0.5(n=4)</b>	<b>2-4(n=111)</b>	<b>4-10 (n=88)</b>	<b>&gt;10 (n=53)</b>
	hsa-miR-33b-5p	hsa-miR-92a-3p	hsa-miR-425-5p
	hsa-miR-4302	hsa-miR-186-5p	hsa-miR-148b-3p
	hsa-miR-486-3p	hsa-miR-424-5p	hsa-miR-139-5p
	hsa-miR-500a-3p	hsa-miR-28-3p	hsa-miR-145-5p
	hsa-miR-30a-3p	hsa-miR-324-3p	hsa-miR-30c-5p
	hsa-miR-550a-5p	hsa-miR-3907	hsa-miR-144-5p
	hsa-miR-627-5p	hsa-let-7i-5p	hsa-miR-331-3p
	hsa-miR-192-5p	hsa-miR-4291	hsa-miR-151a-5p
	hsa-miR-3182	hsa-miR-223-3p	hsa-miR-151a-3p
	hsa-miR-3184-5p	hsa-miR-30e-5p	hsa-miR-142-3p
	hsa-miR-29c-5p	hsa-miR-19a-3p	hsa-miR-30b-5p
	hsa-miR-296-3p	hsa-miR-766-3p	hsa-miR-152-3p
	hsa-miR-1183	hsa-miR-484	hsa-miR-454-3p
	hsa-miR-21-3p	hsa-miR-20b-5p	hsa-miR-26a-5p
	hsa-miR-99b-3p	hsa-miR-197-3p	hsa-let-7a-5p
	hsa-miR-380-5p	hsa-miR-1280	hsa-miR-664a-3p
	hsa-miR-424-3p	hsa-miR-139-3p	hsa-miR-4301
	hsa-miR-1226-3p	hsa-miR-92b-3p	hsa-miR-22-3p
	hsa-miR-26a-1-3p	hsa-miR-1301-3p	
	hsa-miR-302d-5p	hsa-miR-191-3p	
	hsa-miR-1203	hsa-miR-361-5p	
	hsa-miR-661	hsa-miR-182-5p	
	hsa-miR-199a-5p	hsa-miR-590-5p	
	hsa-miR-299-5p	hsa-let-7b-5p	
	hsa-miR-4260	hsa-miR-93-5p	
	hsa-miR-3667-5p	hsa-let-7e-5p	
	hsa-miR-1306-3p	hsa-miR-874-3p	
	hsa-miR-548q	hsa-miR-532-3p	
	hsa-miR-483-5p	hsa-miR-140-3p	
	hsa-miR-26b-3p	hsa-miR-130b-5p	
	hsa-miR-30c-1-3p	hsa-miR-335-5p	
	hsa-miR-24-2-5p	hsa-miR-505-3p	
	hsa-miR-548e-3p	hsa-miR-20a-5p	
	hsa-miR-4274	hsa-miR-15a-5p	
	hsa-miR-3675-3p	hsa-miR-942-5p	
	hsa-miR-29c-3p	hsa-miR-191-5p	
	hsa-miR-23b-5p	hsa-miR-326	

<b>Fold Change</b>			
<b>0.5(n=4)</b>	<b>2-4(n=111)</b>	<b>4-10 (n=88)</b>	<b>&gt;10 (n=53)</b>
	hsa-miR-3180-3p	hsa-miR-93-3p	
	hsa-miR-624-5p	hsa-miR-30d-5p	
	hsa-miR-106b-5p	hsa-miR-340-5p	
	hsa-miR-183-5p	hsa-miR-423-3p	
	hsa-miR-320e	hsa-miR-744-5p	
	hsa-miR-363-3p	hsa-miR-30a-5p	
	hsa-miR-34a-5p	hsa-miR-100-5p	
	hsa-miR-132-3p	hsa-miR-99b-5p	
	hsa-miR-200b-3p	hsa-miR-27b-3p	
	hsa-miR-573	hsa-miR-185-5p	
	hsa-miR-3173-3p	hsa-miR-28-5p	
	hsa-miR-598-3p	hsa-miR-125a-5p	
	hsa-miR-2355-3p	hsa-miR-98-5p	
	hsa-miR-3617-5p	hsa-miR-106b-3p	
	hsa-miR-454-5p	hsa-miR-128-3p	
	hsa-miR-143-3p		
	hsa-miR-20a-3p		
	hsa-miR-181d-5p		
	hsa-miR-125a-3p		
	hsa-miR-7-1-3p		
	hsa-miR-101-3p		
	hsa-miR-543		
	hsa-miR-219a-1-3p		
	hsa-miR-4289		
	hsa-miR-3177-3p		
	hsa-miR-301a-3p		
	hsa-miR-4306		
	hsa-miR-146b-3p		
	hsa-miR-491-5p		
	hsa-miR-142-5p		
	hsa-miR-320a		
	hsa-miR-338-3p		
	hsa-miR-16-5p		
	hsa-miR-720		
	hsa-miR-487b-3p		
	hsa-miR-4326		
	hsa-miR-675-3p		

<b>Fold Change</b>			
<b>0.5(n=4)</b>	<b>2-4(n=111)</b>	<b>4-10 (n=88)</b>	<b>&gt;10 (n=53)</b>
	hsa-miR-155-5p		
	hsa-miR-204-5p		

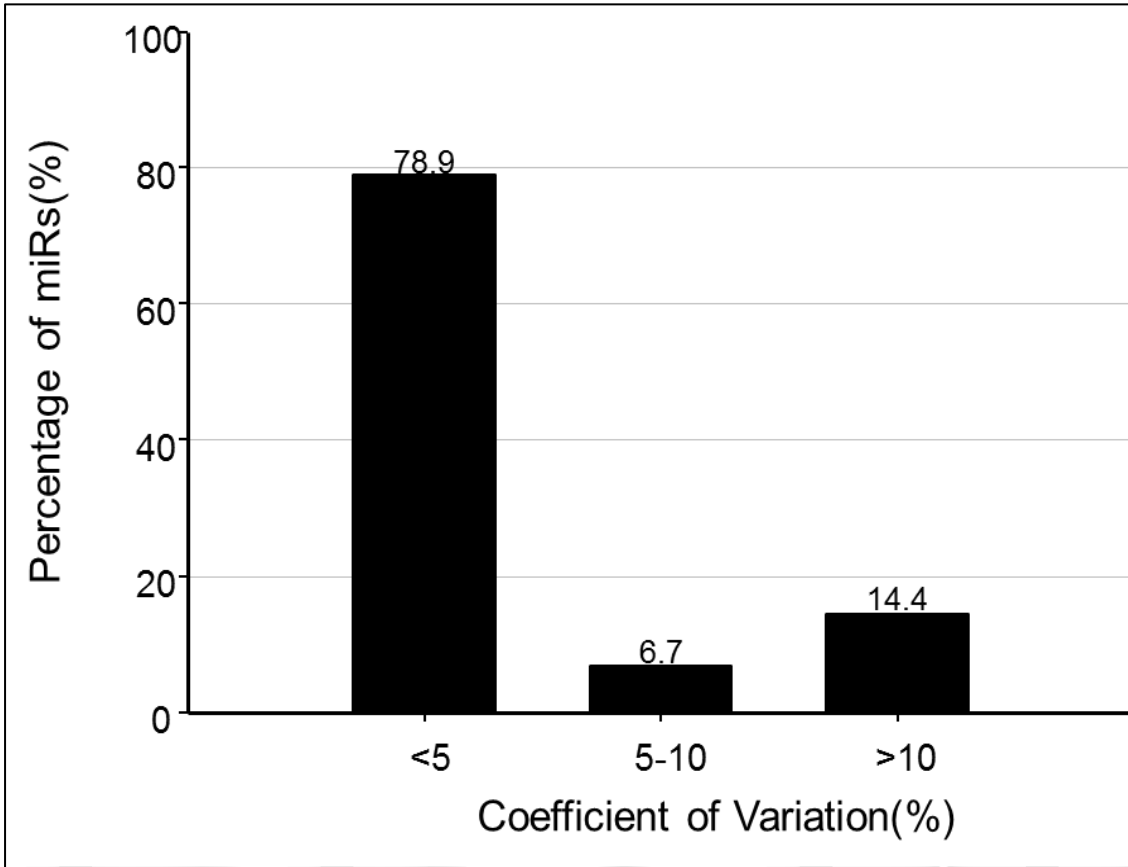


**Figure 3.1: Human Cardiovascular Disease miRNA PCR Array CV Distribution**

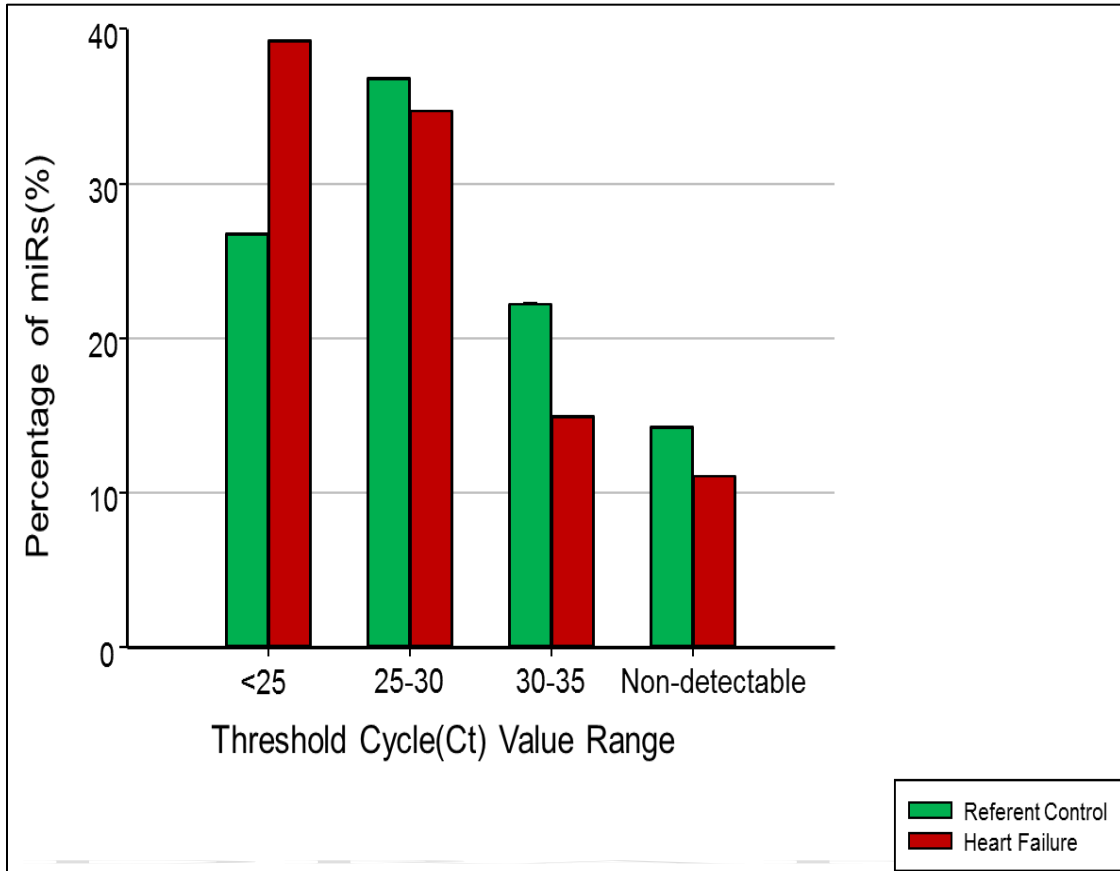


**Figure 3.2: Human Cardiovascular Disease miRNA PCR Array Ct Distribution**

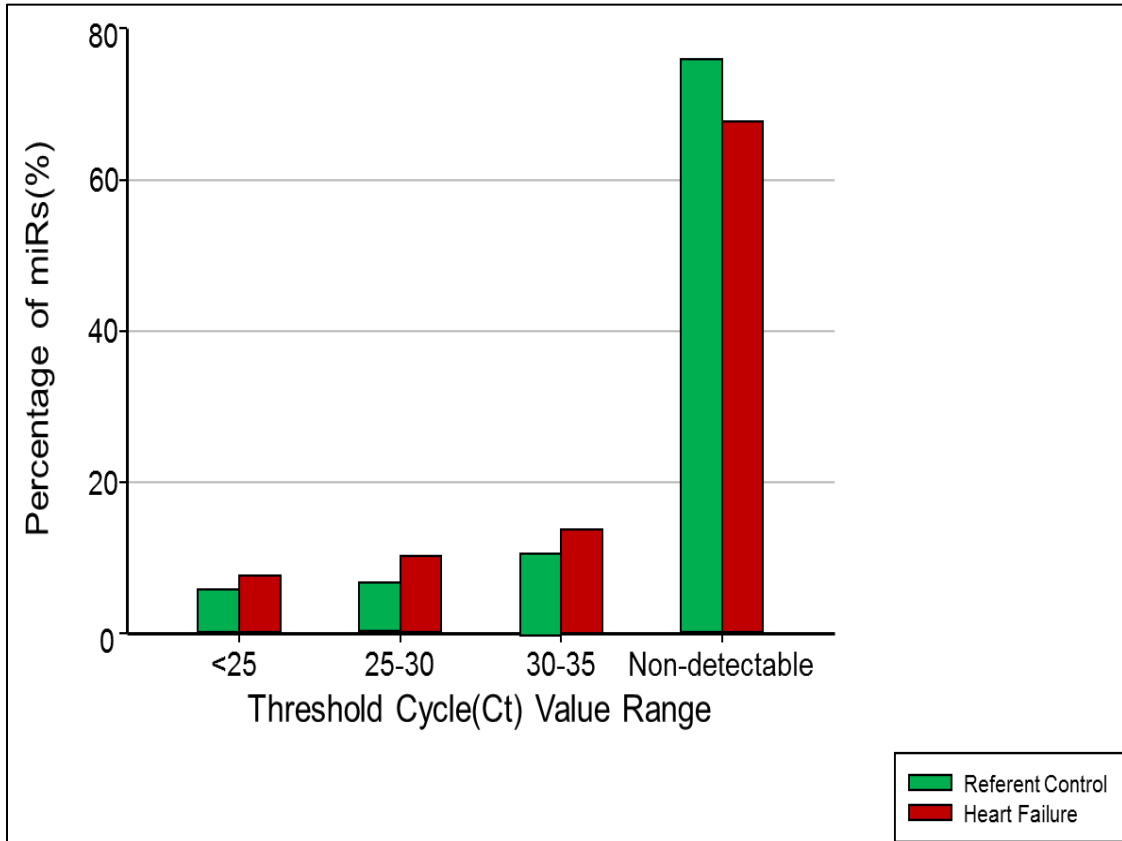


**Figure 3.3: Human miRNome PCR Array PCR Array Ct Distribution**

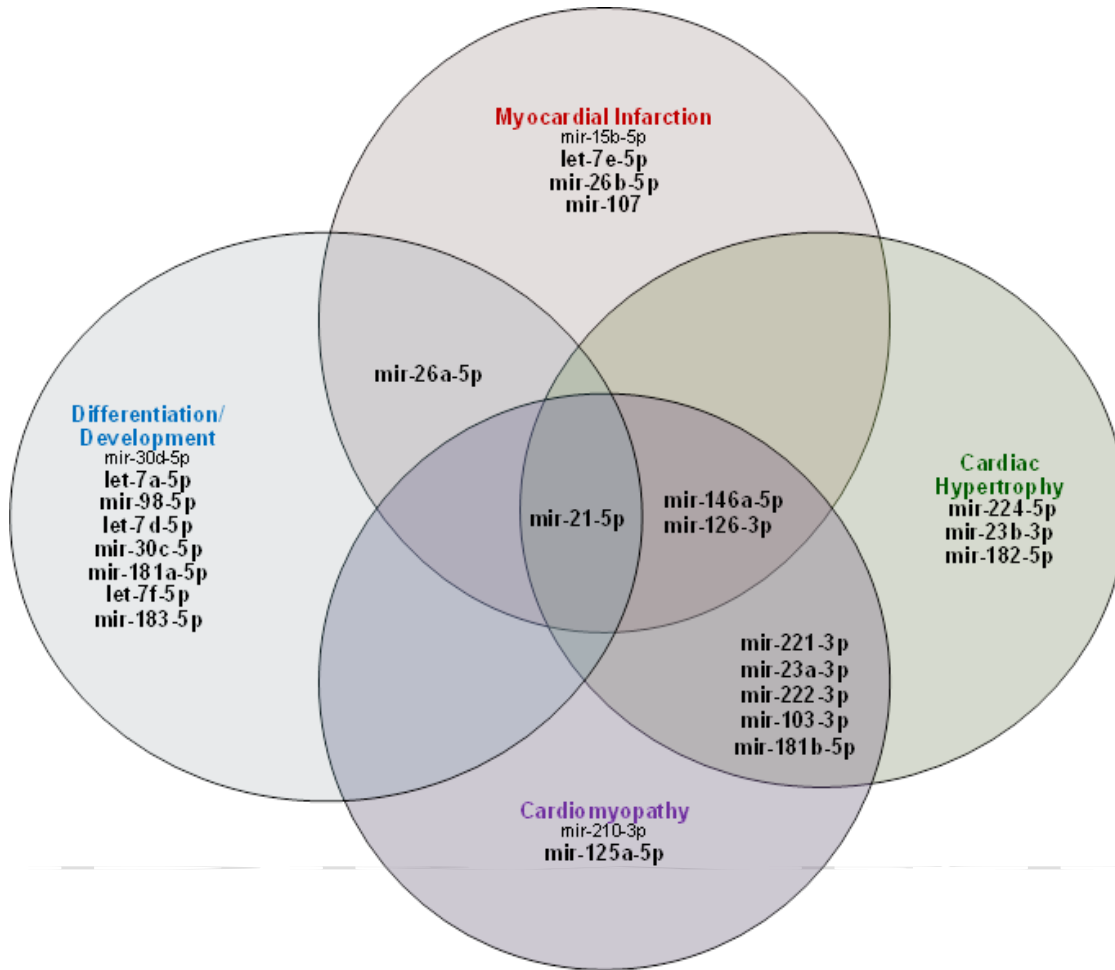


**Figure 3.4: Functional Grouping of miRNAs with >10-fold change.** Venn diagram shows an emerging distinct miRNA profile study with a >10 fold change (HF vs. Referent Control) organized by functional groups. miRNAs listed in the **enlarged bold text** were confirmed to have a fold change on both the Cardiovascular Disease miRNA PCR Array and the miRNome miScript miRNA PCR Array. miRNAs listed in the smaller text only showed a fold change on the Cardiovascular Disease miRNA PCR Array, and not the miRNome miScript miRNA PCR Array.

## CHAPTER 4

### CONCLUSION

#### 4.1 THESIS CONCLUSION

The data gathered from this experiment shows a distinct plasma miRNA biomarker profile emerging between heart failure and referent control groups after optimizing and implementing a standardized, automated protocol for isolating and detecting miRNAs in plasma. With these methods, sample control values maintained low CV values to show high reproducibility when comparing groups. CV values of individual miRNA sequences were able to be monitored and assessed for its performance. These CV values show improvement from previous studies done manually. This indicates less user error occurred and results were more consistent. While extraction efficiency of samples can be improved, the essential outcome is that extraction efficiency remained consistent throughout samples. This consistent nature of sample processing further reduces variability.

Moreover, these automated protocols allowed for higher throughput as time and manual steps were decreased. This allowed for the robust testing of a select PCR panels and entire miRNome testing. **Figure 4.1** shows this automated protocol increases time efficiency by a 6:1 ratio when compared to corresponding manual protocols. While this study serves as a good basis for

future miRNA studies, it also identifies the limitations and areas where optimization is needed.

## 4.2 LIMITATIONS

**Figure 4.2** identifies the areas of optimization needed to improve this protocol and are discussed below.

*Challenge 1:* The initial manual pretreatment step using phenol-chloroform separation serves as a rate-limiting step in this protocol. Furthermore, phenol is a highly corrosive substance and any carryover can have harsh long-term effects on physical platforms.

*Challenge 2:* Endogenous small RNA controls have not been identified in plasma samples. The typical snoRNA/snRNA reference genes listed on the PCR panel are not recommended for data normalization of plasma/serum studies. These snoRNAs/snRNAs have been verified to have relatively invariant expression levels across many cell and tissue types; however, many of them exist in low and varying amounts in normal plasma/serum samples [7,42].

*Challenge 3:* qPCR lacks the sensitivity to quantify low abundant plasma miRNAs and great variation can be seen in these targets even in the replicates of the same sample. While many of the miRNAs were reported with an upregulated fold change on the Cardiovascular panel (**Table 3.1**) also showed the same trend on the miRNome panel (**Table 3.2**), the degree of fold change for some sequences varied widely. This is indicative of lack of precision as qPCR is heavily relies on indirect measurements and environmental conditions to include rate based Ct values and calibration curves.

### 4.3 FUTURE WORK

A new PCR technique is emerging that provides solutions to challenges #2-3. Droplet digital PCR (ddPCR) allows direct absolute quantification of nucleic acids [9,11,46]. This eliminates the need for a reference gene for normalization [10,11,19,30]. Furthermore, it is reported that ddPCR is highly sensitive and is superior to qPCR when measuring miRNAs in low abundance. This is of high importance as miRNAs normally exist in low concentrations in liquid biopsies [11,18,30]. Recent studies reported the lowest copy number detected by ddPCR was 1 copy per ul of input versus 100 copies per ul of input detected by qPCR in the subset of miRNAs tested [30,33].

A ddPCR proof-of-concept test was done with cel-mir-39. These promising results are displayed in **Figure 4.3**. In comparison to RT-qPCR, ddPCR analysis was less labor intensive. Consequently, ddPCR seems to be the future of miRNA quantification and profiling studies.

Along with the utilization of ddPCR, increasing sample patient sizes will be of utmost importance to determine a distinct miRNA profile for HF patients. Also, it is of interest to compare freely circulating miRNA profiles, exosomal miRNA profiles, and whole blood profiles in the future. Of particular interest is whole blood collected via PAXgene Blood RNA tubes. PAXgene tubes allows for immediate stabilization of blood intracellular RNA to preserve the gene expression profile. This could prevent dysregulation of RNA immediately after blood is drawn and avoid transferring errors of samples to various tubes such as EDTA, serum, etc.

This study identifies a standardized, high-throughput protocol that can be used as a springboard to optimize miRNA profiling studies to be used as a diagnostic tool in a wide range of diseases.

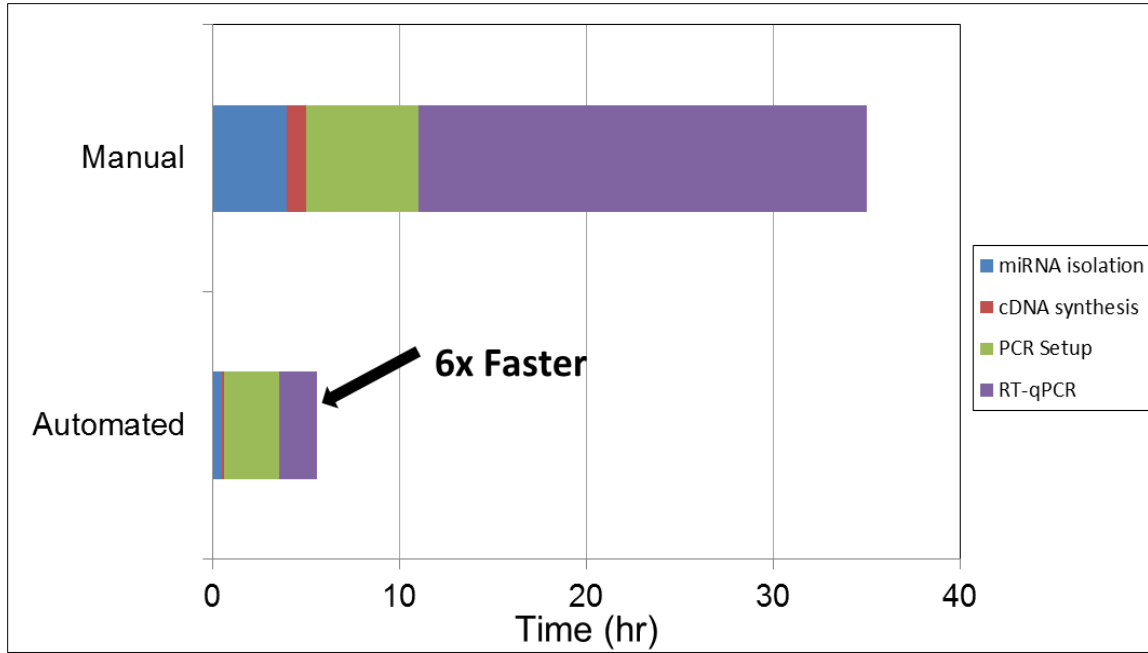


**Figure 4.1: Manual Vs Automated Protocol-Time Efficiency.** Manual Protocol: Actual time shown to process 12 total samples. Automated: Time shown as efficiency ratio (in comparison to manual) to process 12 total samples.

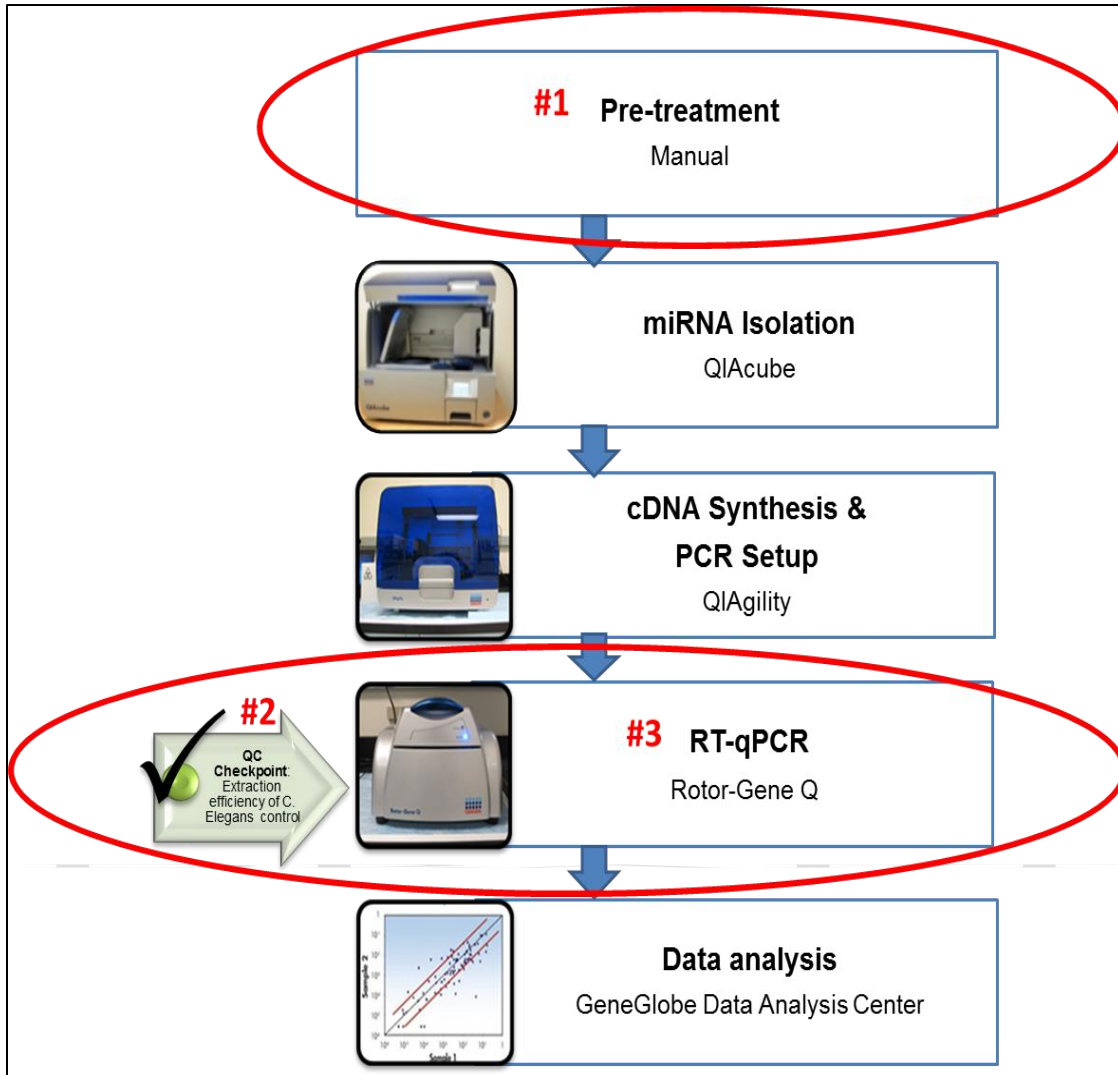


**Figure 4.2: RT-qPCR Workflow Challenges.** Challenging points indicated by red circle and red number from top to bottom of workflow. Challenge **#1**: Manual pretreatment. Challenge **#2**: No endogenous controls for normalization. Challenge **#3**: Indirect Ct measurements of qPCR.

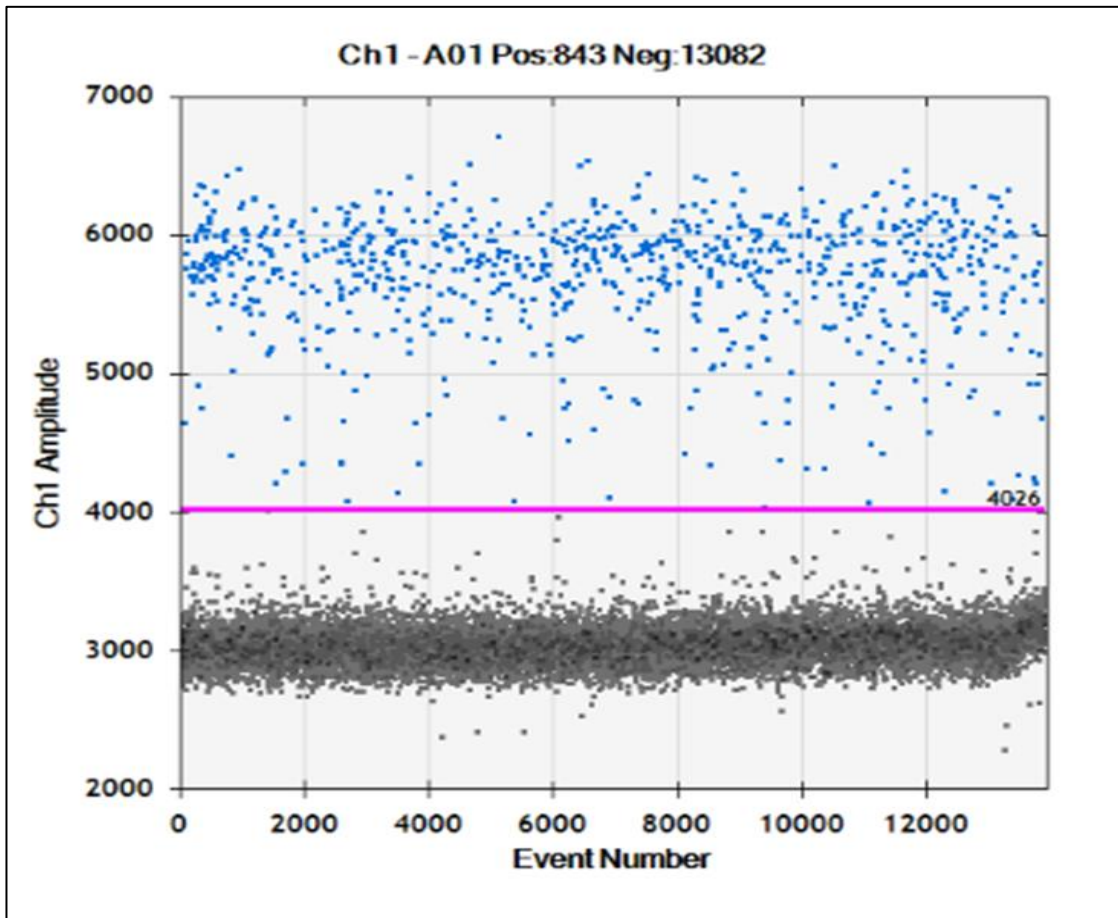


**Figure 4.3: ddPCR Proof-of-concept.** Image shows representative well count of C-elegans mir-39-3p as a standard. **Pink line** indicates threshold. **Blue dots** above threshold indicate count of positive droplets that contain at least one miRNA copy. **Gray dots** below threshold indicate count of negative droplets. The clustering of negative and positive droplets, respectively, with sufficient separation between indicates a well performed assay.

## REFERENCES

1. Accerbi M, et al. Methods for isolation of total RNA to recover miRNAs and other small RNAs from diverse species. *Methods in molecular biology*. 2010;592:31–50.
2. Akat KM, Moore-McGriff D, Morozov P, Brown M, Gogakos T, Da Rosa JC, et al. Comparative RNA-sequencing analysis of myocardial and circulating small RNAs in human heart failure and their utility as biomarkers. *PNAS*. 2014; 111:11151-11156.
3. Ambros V. The functions of animal microRNAs. *Nature*. 2004;431:350–355.
4. Arroyo JD, et al. Argonaute2 complexes carry a population of circulating microRNAs independent of vesicles in human plasma. *Proc Natl Acad Sci U S A*. 2011;108:5003–8.
5. Callis T.E., Pandya K., Seok H.Y., Tang R.H., Tatsuguchi M., Huang Z.P., Chen J.F., Deng Z., Gunn B., Shumate J., et al. MicroRNA-208a is a regulator of cardiac hypertrophy and conduction in mice. *J. Clin. Investig*. 2009;119:2772–2786.
6. Carè A, Catalucci D, Felicetti F, et al. MicroRNA-133 controls cardiac hypertrophy. *Nat Med*. 2007;13:613–618.
7. Chim SS, et al. Detection and characterization of placental microRNAs in maternal plasma. *Clin Chem*. 2008;54:482–90.

8. Christenson R.H., Azzazy H.M., Duh S.H., Maynard S., Seliger S.L., Defilippi C.R. Impact of increased body mass index on accuracy of B-type natriuretic peptide (BNP) and N-terminal proBNP for diagnosis of decompensated heart failure and prediction of all-cause mortality. *Clin. Chem.* 2010;56:633–641.
9. Diehl F, Diaz LA. Digital quantification of mutant DNA in cancer patients. *Curr Opin Oncol.* 2007;19(1):36–42.
10. Dingle TC, Sedlak RH, Cook L, Jerome KR. Tolerance of droplet-digital PCR vs real-time quantitative PCR to inhibitory substances. *Clin Chem.* 2013;59:1670–2.
11. El-Khoury, V., Pierson, S., Kaoma, T., Bernardin, F., & Berchem, G. Assessing cellular and circulating miRNA recovery: the impact of the RNA isolation method and the quantity of input material. *Scientific Reports.* 2016; 6: 19529.
12. Enderle D, Spiel A, Coticchia CM, Berghoff E, Mueller R, Schlumpberger M, et al.. Characterization of RNA from Exosomes and Other Extracellular Vesicles Isolated by a Novel Spin Column-Based Method. *PLoS ONE.* 2015; 10(8): e0136133.
13. Fuat A., Murphy J.J., Hungin A.P., Curry J., Mehrzad A.A., Hetherington A., Johnston J.I., Smellie W.S., Duffy V., Cawley P. The diagnostic accuracy and utility of a B-type natriuretic peptide test in a community population of patients with suspected heart failure. *Br. J. Gen. Pract.* 2006;56:327–333.
14. Fukushima Y., Nakanishi M., Nonogi H., Goto Y., Iwai N. Assessment of plasma miRNAs in congestive heart failure. *Circ. J.* 2011;75:336–340.

15. Goyal A., Norton C.R., Thomas T.N., Davis R.L., Butler J., Ashok V., Zhao L., Vaccarino V., Wilson P.W. Predictors of incident heart failure in a large insured population: A one million person-year follow-up study. *Circ. Heart Fail.* 2010;3:698–705.
16. Griffiths-Jones S, Grocock RJ, van Dongen S, Bateman A, Enright AJ. miRBase: microRNA sequences, targets and gene nomenclature. *Nucleic acids research.* 2006;34:D140–4.
17. Hausser J., Zavolan M. Identification and consequences of miRNA-target interactions—Beyond repression of gene expression. *Nat. Rev. Genet.* 2014;15:599–612.
18. Hindson BJ, Ness KD, Masquelier DA, et al. High-throughput droplet digital PCR system for absolute quantitation of DNA copy number. *Anal Chem.* 2011;83(22):8604–10.
19. Hindson CM, Chevillet JR, Briggs HA, Gallichotte EN, Ruf IK, Hindson BJ, et al. Absolute quantification by droplet digital PCR versus analog real-time PCR. *Nat Methods.* 2013;10:1003-5.
20. Hogg K., Swedberg K., McMurray J. Heart failure with preserved left ventricular systolic function; epidemiology, clinical characteristics, and prognosis. *J. Am. Coll. Cardiol.* 2004;43:317–327.
21. Hunter MP, Ismail N, Zhang X, Aguda BD, Lee EJ, Yu L, Xiao T, Schafer J, Lee ML, Schmittgen TD, Nana-Sinkam SP, Jarjoura D, Marsh CB. Detection of microRNA expression in human peripheral blood microvesicles. *PLoS One.* 2008;3:e3694.

22. Kim V.N., Han J., Siomi M.C. Biogenesis of small RNAs in animals. *Nat. Rev. Mol. Cell Biol.* 2009;10:126–139.
23. Klip I.T., Voors A.A., Anker S.D., Hillege H.L., Struck J., Squire I., van Veldhuisen D.J., Dickstein K., investigators O. Prognostic value of mid-regional pro-adrenomedullin in patients with heart failure after an acute myocardial infarction. *Heart.* 2011;97:892–898.
24. Kozomara A., Griffiths-Jones S. MiRBase: Annotating high confidence microRNAs using deep sequencing data. *Nucleic Acids Res.* 2014;42:D68–D73.
25. Kroh EM, Parkin RK, Mitchell PS, Tewari M. Analysis of circulating microRNA biomarkers in plasma and serum using quantitative reverse transcription-PCR (qRT-PCR). *Methods.* 2010;50:298–301.
26. Kumarswamy R, Thum, T. Non-coding RNAs in Cardiac Remodeling and Heart Failure. *Circ Res.* 2013; 113:676-689.
27. Lee Y., Kim M., Han J., Yeom K.H., Lee S., Baek S.H., Kim V.N. MicroRNA genes are transcribed by RNA polymerase II. *EMBO J.* 2004;23:4051–4060.
28. Leuschner P.J., Ameres S.L., Kueng S., Martinez J. Cleavage of the siRNA passenger strand during RISC assembly in human cells. *EMBO Rep.* 2006;7:314–320.
29. Lu J, et al. MicroRNA expression profiles classify human cancers. *Nature.* 2005;435:834–8.
30. Ma, J., Li, N., Guarnera, M., & Jiang, F. Quantification of Plasma miRNAs by Digital PCR for Cancer Diagnosis. *Biomarker Insights.* 2013; 8:127–136.

31. McMurray J.J., Adamopoulos S., Anker S.D., Auricchio A., Bohm M., Dickstein K., Falk V., Filippatos G., Fonseca C., Gomez-Sanchez M.A., et al. ESC guidelines for the diagnosis and treatment of acute and chronic heart failure 2012: The Task Force for the Diagnosis and Treatment of Acute and Chronic Heart Failure 2012 of the European Society of Cardiology. Developed in collaboration with the Heart Failure Association (HFA) of the ESC. *Eur. J. Heart Fail.* 2012;14:803–869
32. Meiliana A, Wijaya, Andi. MicroRNAs in Cardiometabolic Diseases. *Indones Biomed J.* 2013; 5:67-80.
33. Miotto E, Saccenti E, Lupini L, Callegari E, Negrini M, Ferracin M. Quantification of circulating mirnas by droplet digital PCR: comparison of evagreen- and taqman-based chemistries. *Cancer Epidemiol Biomarkers Prev.* 2014;23:2638–42.
34. Peltier HJ, Latham GJ. Normalization of microRNA expression levels in quantitative RT-PCR assays: identification of suitable reference RNA targets in normal and cancerous human solid tissues. *RNA.* 2008;14:844–52.
35. Pillai R.S. MicroRNA function: Multiple mechanisms for a tiny RNA? *RNA.* 2005;11:1753–1761.
36. Pritchard CC, Chang HH, Muneesh T. MicroRNA profiling: approaches and consideration. *Nat Rev Genet.* 2015; 13:358-369.
37. Richards A.M. The natriuretic peptides in heart failure. *Basic Res. Cardiol.* 2004;99:94–100.

38. Richards M., Di Somma S., Mueller C., Nowak R., Peacock W.F., Ponikowski P., Mockel M., Hogan C., Wu A.H., Clopton P., et al. Atrial fibrillation impairs the diagnostic performance of cardiac natriuretic peptides in dyspneic patients: Results from the BACH Study (Biomarkers in ACute Heart Failure). *JACC Heart Fail.* 2013;1:192–199.
39. Rodriguez A., Griffiths-Jones S., Ashurst J.L., Bradley A. Identification of mammalian microRNA host genes and transcription units. *Genome Res.* 2004;14:1902–1910.
40. Rosenfeld N, et al. MicroRNAs accurately identify cancer tissue origin. *Nature biotechnology.* 2008;26:462–9.
41. Sayed AS, Xia K, Yang T, Peng J. Circulating microRNAs: A potential role in diagnosis and prognosis of acute myocardial infarction. *Disease Markers.* 2013; 35:561-566.
42. Tiberio P, Callari M, Angeloni V, Daidone MG, Appierto V. Challenges in using circulating miRNAs as cancer biomarkers. *Biomed Res Int.* 2015;2015:731479.
43. Van Veldhuisen D.J., Linssen G.C., Jaarsma T., van Gilst W.H., Hoes A.W., Tijssen J.G., Paulus W.J., Voors A.A., Hillege H.L. B-type natriuretic peptide and prognosis in heart failure patients with preserved and reduced ejection fraction. *J. Am. Coll. Cardiol.* 2013;61:1498–1506.
44. Vegter EL, van der Meer P, de Windt LJ, Pinto YM, Voors AA. MicroRNAs in heart failure: from biomarker to target for therapy. *European Journal of Heart Failure.* 2016; 18:457-468.

45. Vickers KC, Palmisano BT, Shoucri BM, Shamburek RD, Remaley AT. MicroRNAs are transported in plasma and delivered to recipient cells by high-density lipoproteins. *Nat Cell Biol* 2011;13:423–433.
46. Vogelstein B, Kinzler KW. Digital PCR. *Proc Natl Acad Sci USA*. 1999;96(16): 9236–41.
47. Wang K, Zhang S, Weber J, Baxter D, Galas DJ. Export of microRNAs and microRNA-protective protein by mammalian cells. *Nucleic Acids Res*. 2010;38:7248–7259.
48. Wei X.J., Han M., Yang F.Y., Wei G.C., Liang Z.G., Yao H., Ji C.W., Xie R.S., Gong C.L., Tian Y. Biological significance of miR-126 expression in atrial fibrillation and heart failure. *Braz. J. Med. Biol. Res*. 2015;48:983–989.
49. Wong LL, Wang J, Liew OW, Richard AM, Chen Y. MicroRNA and Heart Failure. *Int. J. Mol. Sci*. 2016; 17,502.
50. Yancy C.W., Jessup M., Bozkurt B., Butler J., Casey D.E., Jr., Drazner M.H., Fonarow G.C., Geraci S.A., Horwich T., Januzzi J.L., et al. 2013 ACCF/AHA guideline for the management of heart failure: Executive summary: A report of the American College of Cardiology Foundation/American Heart Association Task Force on practice guidelines. *Circulation*. 2013;128:1810–1852.
51. Zile MR, Mehurg SM, Arroyo JE, Stroud RS, DeSantis SM, Spinale FG. Relationship between the temporal profile of plasma microRNA and left ventricular remodeling in patients after myocardial infarction. *Circ Cardiovascular Genet*. 2011; 4:614-619.